J Therm Anal Calorim (2014) 115:2171–2178
DOI 10.1007/s10973-013-3598-x

Thermal stability and folding kinetics analysis of disordered protein, securin

Hsueh-Liang Chu · Tzu-Hsuan Chen · Chang-You Wu · Yao-Chen Yang · Shin-Hua Tseng · Tsai-Mu Cheng · Li-Ping Ho · Li-Yun Tsai · Hsing-yuan Li · Chia-Seng Chang · Chia-Ching Chang

Received: 29 May 2013 / Accepted: 15 December 2013 / Published online: 8 January 2014

Abstract Lacking a stable tertiary structure, intrinsically disordered proteins (IDPs) possess particular functions in cell regulation, signaling, and controlling pathways. The study of their unique structural features, thermal stabilities, and folding kinetics is intriguing. In this study, an identified IDP, securin, was used as a model protein. By using a quasi-static five-step (on-path) folding process, the function of securin was restored and analyzed by isothermal titration calorimetry. Fluorescence spectroscopy and particle size analysis indicated that securin possessed a compact hydrophobic core and particle size. The glass transition of securin was characterized using differential scanning microcalorimetry. Furthermore, the folding/unfolding rates (k_{obs}) of securin were undetectable, implying that the folding/unfolding rate is very fast and that the conformation of securin is sensitive to solvent environmental change. Therefore, securin may fold properly under specific physiological conditions. In summary, the thermal glass transition behavior and undetectable k_{obs} of folding/unfolding reactions may be two of the indices of IDP.

Keywords Securin · Disordered protein · Thermal stability · Folding kinetics

H.-L. Chu · T.-H. Chen · C.-Y. Wu · Y.-C. Yang · S.-H. Tseng · T.-M. Cheng · L.-P. Ho · H. Li · C.-C. Chang (✉)
Department of Biological Science and Technology, National Chiao Tung University, Hsinchu 30050, Taiwan
e-mail: ccchang01@faculty.nctu.edu.tw

T.-H. Chen · C.-S. Chang · C.-C. Chang
Institute of Physics, Academia Sinica, Taipei 11529, Taiwan

T.-M. Cheng
Graduate Institute of Translational Medicine, College of Medicine and Technology, Taipei Medical University, Taipei 11031, Taiwan

L.-Y. Tsai
Institute of Biomedical Sciences, Academia Sinica, Taipei 11529, Taiwan

Introduction

Intrinsically disordered proteins (IDPs) or intrinsically disordered (ID) regions are characterized by the unique combination of high specificity and low affinity in their interactions with functional partners [1]. These proteins or regions lack specific three-dimensional structures [2]. However, ID regions may exist in proteins that have secondary structures, such as p53 [3] and BRCA1 [4]. Moreover, the thermal stability and folding kinetics of these "natively unfolded" [5], "intrinsically disordered" [6], or "intrinsically unstructured" [2] proteins remain ambiguous. It is, therefore, intriguing to identify the structural features and folding kinetics of IDPs.

Human securin (pituitary tumor-transforming gene, PTTG1) is identified as an IDP [7] and has been shown to possess multiple biological functions [8–12]. The expression level of securin corresponds to tumor invasion [13]. During the cell cycle, securin can bind to separase and inhibit the separation of sister chromatin. Securin is the target of the anaphase-promoting complex and is degraded before entering anaphase by polyubiquitination, which depends on the destruction sequences [14]. Additionally, securin is also involved in DNA damage repair [12] and metabolism [15]. Securin can also bind to p53 and inhibit its transcriptional activity to reduce p53-induced cell death [16]. These multifunctional features of IDP may relate to the structural flexibility of its tertiary structure [17].

In this study, we cloned the human securin gene and expressed the protein in an *Escherichia coli* expression system. The expressed human securin was refolded and its function was recovered by a quasi-static five-step (or on-path, over-critical) folding process [18–24].

Moreover, stable molten globule intermediates were observed during this process. Particle size, intrinsic fluorescence, and secondary structure of these folding reaction intermediates of securin were analyzed by dynamic light scattering (DLS) analysis, fluorospectrophotometry, and circular dichroism (CD), respectively. These results indicate that securin is an IDP with a compact hydrophobic core and particle size. Differential scanning microcalorimetry (DSC) results indicate that securin has very weak tertiary interactions. Kinetic studies of the unfolding/folding reactions of securin indicate that both the folding and unfolding rates are too fast to be detected. However, the hysteresis behavior of the securin folding/unfolding reactions at equilibrium indicates that the folding and unfolding reaction may not be a simple two-state reaction.

Materials and methods

Materials and buffers

All chemicals were purchased from Merck Ltd. (Rahway, NJ). The BL21(DE3) cells and the pET200 vector were purchased from Invitrogen (Carlsbad, CA). Primers were synthesized by Biokit (MiaoLi, Taiwan). Human recombinant p53 was cloned from CHO cells, as described in the previous studies [25]. All components of the unfolding buffer and each folding buffer are modified from the previous studies [20, 22, 24] and listed in Table 1.

Cloning and expression of recombinant human securin

The human securin gene was amplified from the A549 cell line and cloned into the pET200 vector by using the polymerase chain reaction with the following primers, securin forward primer: 5′-*CACCCATATGGCTACTCTGA TCTATGTT*-3′ and securin reverse primer: 5′-*ATTTAAA TATCTATGTCACAGCA*-3′.

The constructed plasmid was transformed into BL21(DE3) cells. *E. coli* with the recombinant human securin gene was incubated with shaking at 37 °C, induced with 1 mM IPTG for 16 h, and then centrifuged at 12,000×*g* for 5 min. The cell pellet was resuspended in 3 mL of ddH_2O and disrupted by a cell disruptor (Constant System Ltd., Northants, UK). The total cell lysate was centrifuged at 12,000×*g* for 5 min. The inclusion bodies, which contained securin, were collected and washed with ice-cold ddH_2O twice. The recombinant securin protein was purified by His GraviTrap column (GE Healthcare Bio-Sciences Corp., Piscataway, NJ).

Unfolding and folding of recombinant securin in various folding reaction

Purified securin was dissolved with unfolding buffer to a concentration of 10 mg mL^{-1}. In order to reveal the folding reaction in different folding path, three different folding reactions were tested: direct dilution (off-path reaction), single-step dialysis, and five-step (path dependent or on-path) quasi-static folding process [18–24]. For the off-path process, unfolded securin was directly dropped into tenfold native buffer, mixed well at ambient temperature, and incubated for 1 h until the reaction reached equilibrium. The residual denaturant in the off-path folding reaction buffer was removed by Amicon Ultra (Millipore Corporation, Billerica, MA) centrifugation at 12,000×*g* for 30 min. Next, 700 μL of the native buffer was added to the concentrated sample and centrifuged (12,000×*g*, 30 min) ten times. For single-step dialysis, 1 mL of unfolded securin protein was dialyzed against 500 mL native buffer for 8 h (4 times) to remove the denaturant in solution. For the on-path (five-step) quasi-static folding process [18–24], five folding buffers (listed in Table 1) were used sequentially at 4 °C, and stable reaction intermediates M_1–M_5 were obtained.

Intrinsic fluorescence analysis of securin

Intrinsic fluorescence (emitted by the aromatic residues Trp, Phe, and Tyr) of folded securin, obtained from different folding paths, has been investigated. Fluorescence

Table 1 Chemical compositions of unfolding and refolding buffer

	Tris buffer/mM	pH	Urea/M	DTT/mM	Mannitol/%	Pefabloc/μM
Unfolding buffer	10	11	4.5	1	0.1	5
Folding buffer 1	10	11	2	0.1	0.1	0.5
Folding buffer 2	10	11	1	0.1	0.1	0.5
Folding buffer 3	10	11	–	0.1	0.1	0.5
Folding buffer 4	10	8.8	–	0.1	0.1	0.5
Folding buffer 5	10	8.8	–	0.1	–	0.5

spectra were recorded with a Hitachi F-7000 fluorescence spectrophotometer (Hitachi High Technologies, Tokyo, Japan) using a 1-cm cuvette at 25 °C. The aromatic residues of securin were excited at 280 nm, and the emission spectrum was recorded in the range of 300–450 nm with a 290-nm long-pass filter.

Isothermal titration calorimetry (ITC) analysis of the binding between securin and p53

ITC has been used in many studies to analyze protein–protein or protein–ligand interactions, such as that of apo-human transferrin with sodium *n*-dodecyl sulfate [26]. A 2277 Thermal Activity Monitor (TAM, ThermoMetric AB, Sweden) was used to determine the binding constant, K_a, and reaction enthalpy, ΔH, for the binding of p53 to securin. A 10 μM securin solution was dissolved in Tris buffer (10 mM, pH = 8.8) to a final volume of 2.8 mL. The mixture was placed into the measuring ampule and titrated by adding 10 μL drops of a 300 μM p53 solution, with an injection rate of 1 μL s^{-1}; the interval between two consecutive portions is 15 min. Finally, 200 μL of p53 solution was added into the measuring ampule. A temperature of 25 °C was maintained throughout the experiment.

Analysis of the intermolecular interaction between securin and p53 using the far-western blot technique

Recombinant securin and p53 were unfolded and resolved by 14 % SDS-PAGE and then electrotransferred onto a polyvinylidene difluoride (PVDF) membrane (Millipore Corporation, Billerica, MA) with a semi-dry transfer blotter (ATTO Corporation, Tokyo, Japan). These proteins were refolded on the PVDF membrane by a modified on-path refolding process, and the buffers were sequentially changed from folding buffer 1 to folding buffer 5 (Table 1) [20, 22, 24]. The membrane was washed twice in each buffer for 5 min, and then incubated in blocking solution (10 mM Tris, 100 mM NaCl, 0.1 % Tween-20, 5 % nonfat milk, pH = 7.5) for 30 min at room temperature. For the far-western blot analysis, after incubating the transferred membrane in the blocking solution, refolded human recombinant securin (10 μg mL^{-1} in R_5 buffer) was added, and the membrane was gently shaken for 2 h at 37 °C. The recombinant securin was detected using a mouse anti-securin antibody (Abcam, Cambridge, UK) that was recognized by a horseradish peroxidase (HRP)-conjugated goat anti-mouse secondary antibody. Chemiluminescent HRP substrates (Millipore Corporation, Billerica, MA) were used to enhance the chemiluminescence signal. Bovine serum albumin was used as a negative control.

Inspection of securin particle size by DLS

Dynamic light scattering measurements were made using a goniometer from Brookhaven Instruments Corp. (BIC, Holtsville, NY), including a diode-pumped laser (Coherent, Santa Clara, CA) with a wavelength of 532.15 nm and power of 10 mW. The scattered light was collected at 90° from the incident direction. The chamber temperature was kept at 20 °C using a water circulator. The autocorrelation function was computed using a digital correlator (BI 9000, BIC, Holtsville, NY) and then analyzed by the negatively constructed least-squares method [27].

CD analysis of securin secondary structure

Circular dichroism spectra in the far UV region (260–200 nm) of U and M_{1-5} were measured using a Jasco J 720C spectropolarimeter (Jasco Ltd., Tokyo, Japan) at 20 °C with a 0.1-cm cuvette. The mean residue ellipticity, θ_{MRE} (deg cm^2 $dmol^{-1}$ $residue^{-1}$), was calculated from the molecular mass and number of residues of securin (M.W. = 24.703 kDa; 225 amino acids).

Thermal stability of securin monitored by DSC

N-DSC II (Calorimetry Sciences Corporation, CSC, Lindon, UT) was used for experiments on the thermal stability of securin. The collected data were then analyzed by an automatic data collection program. Each sample was adjusted to 2 mg mL^{-1}. BSA was used as a control for regular protein. All samples were filtered and degassed under vacuum for 5–10 min, with gentle stirring, before being placed into the calorimetry cell. DSC experiments were performed at a constant pressure of 4 atm to avoid bubble formation. The temperature of the samples increased at a constant heating rate of 0.5 °C min^{-1}. The excess heat capacity was calculated using the CpCalc program (Calorimetry Sciences Corporation, CSC, Lindon, UT).

Measurement of the kinetic unfolding/folding rate constant of securin

Stopped-flow unfolding and folding experiments of securin were performed with an Aviv model 202SF stopped-flow CD and fluorescence spectrophotometer (Aviv Biomedical, Lakewood, NJ), equipped with a thermoelectric cell holder at 25 °C. The dead time for mixing was 100 μs. All of these experiments were performed using a 0.1-cm cuvette. Unfolding jumps were from 0 M urea to various concentrations of urea (0.5–8 M); folding jumps were performed from 8 M urea to various urea concentrations (7.5–0 M).

Determination of protein stability in the unfolding/folding equilibrium reaction

In this experiment, 100 μL of unfolded or folded securin protein was diluted into 1 mL urea-containing buffer. Unfolding experiments were performed from 0 M urea to various concentrations of urea (0.5–8 M); folding experiments were performed from 8 M urea to various urea concentrations (7.5–0 M). The mixed samples were incubated at 4 °C overnight to ensure complete equilibration. Fluorescence spectra were recorded with a Hitachi F-7000 fluorescence spectrophotometer (Hitachi High Technologies, Tokyo, Japan), using a 1-cm cuvette at 25 °C. The protein solutions were excited at 280 nm, and the emission at 300–450 nm was recorded at 90° relative to the excitation, with a 5-nm bandwidth and a 290 nm long-pass filter. ΔG between the unfolded and folded states of the securin protein can be calculated by the following equation [28].

$$\Delta G_{\mathrm{f-u}}^{\mathrm{H_2O}} = -m_{\mathrm{f-u}}[\mathrm{urea}]_{50\,\%}, \quad (1)$$

where $m_{\mathrm{f-u}}$ is the m-value, which can be calculated by the following equation.

$$m = \partial(\Delta G_{\mathrm{f-u}}([\mathrm{urea}]))/\partial[\mathrm{urea}], \quad (2)$$

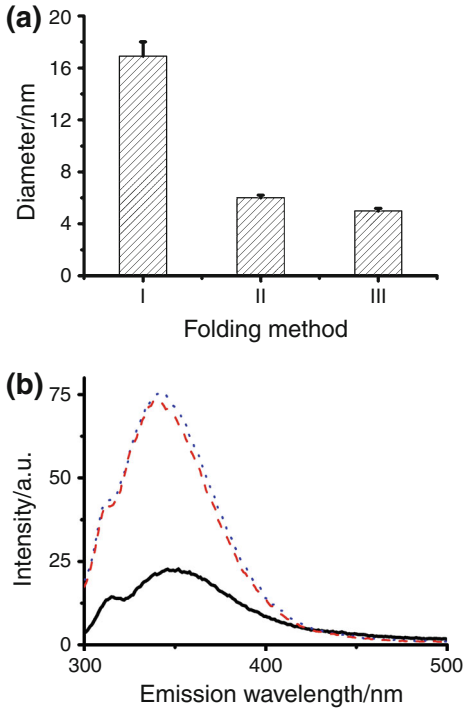

Fig. 1 Particle size and intrinsic fluorescence analysis of the securin protein via different folding paths. **a** Particle size analysis of securin by DLS. **b** Intrinsic fluorescence analysis by fluorescence spectrophotometry. Folding methods I, II, and III denote the direct dilution (off-path folding), single-step dialysis, and five-step (on-path) folding process, respectively

where $[\mathrm{urea}]_{50\,\%}$ is the urea concentration at the midpoint of the equilibrium between the folded and unfolded states.

Results

Particle sizes and intrinsic fluorescence of the securin protein in different folding paths

According to DLS analysis, the particle sizes of refolded securin, which were obtained from off-path, single-step dialysis, and on-path folding paths, were 16.9 ± 1.1, 6 ± 0.2, and 5 ± 0.2 nm, respectively (Fig. 1a). The smallest particle size, which indicated the most compact conformation, of refolded securin was obtained from the on-path folding process. Similar results were obtained from intrinsic fluorescence measurements. In the protein folding process, hydrophobic collapse would lead to a blueshift in the fluorescence maximum (λ_{max}) [29]. Thus, the shortest λ_{max} value could indicate the most compact hydrophobic

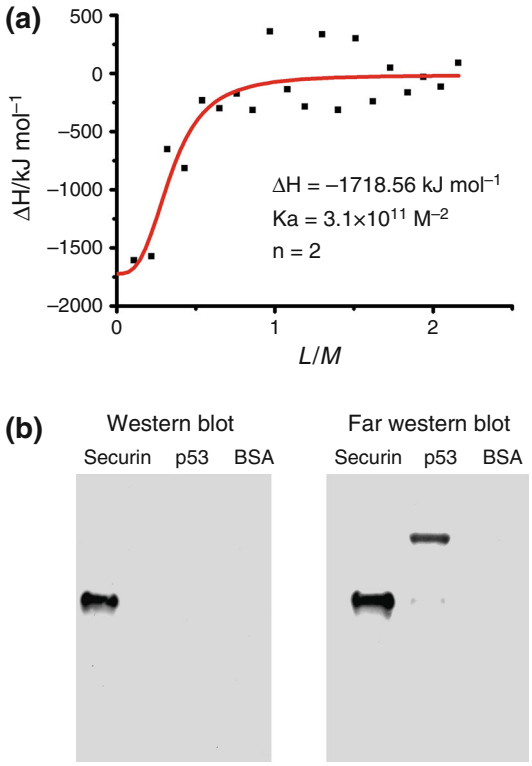

Fig. 2 **a** Analysis of the binding between securin and p53. The enthalpy change (ΔH) for the binding of securin to p53 is equal to -1718.56 kJ mol^{-1}. In the figure, [L] represents the concentration of p53 and [M] represents the concentration of securin. The binding ratio of p53 and securin is 1–2. **b** Identification of securin by western blot analysis with an anti-securin monoclonal antibody after the expression of securin and p53 in BL21 cell lines (*left*), with BSA used as a negative control. The interaction of securin and p53 was demonstrated by far-western blot analysis (*right*)

core [29]. In Fig. 1b, λ_{max} of the intrinsic fluorescence of securin was obtained from the on-path folding process and single-step dialysis method, but not from the off-path folding method. Accordingly, securin was sensitive to the folding path, and the protein obtained from the on-path folding process was the most stable. Therefore, we focused on folded securin prepared by the on-path folding process in the following experiments.

Binding assay of securin and p53

As described in a previous study, securin can directly interact with p53 [16]. In this study, the interaction between securin and p53 was investigated by ITC measurements and far-western analyses to evaluate whether securin folded into functional state or not. (Fig. 2). Based on ITC measurements, the binding constant, K_a, between securin and p53 was found to be $3.1 \times 10^{11}\ M^{-2}$, the ΔH was $-1{,}718.56$ kJ mol^{-1}, and the molar ratio of binding between p53 and securin was 1:2 (Fig. 2a). These results indicate that the folded securin protein could bind directly to p53. In addition, far-western blot analysis (Fig. 2b) revealed that securin could bind to its interaction partner, p53, but not to the negative control, BSA. Thus, functional securin could be obtained from the on-path folding process.

Intrinsic fluorescence, particle size, and secondary structure analyses of folded and folding reaction intermediates of securin

The intrinsic fluorescence spectra of reaction intermediates of securin (Fig. 3a) were analyzed to reveal the dynamics of hydrophobic core formation in the protein. The fluorescence intensity increased with the progression of the folding reaction ($M_5 > M_4 > M_3 > M_2 > M_1 > U$). The emissions, λ_{max}, of the intrinsic fluorescence of securin intermediates from unfolding to folded were 348, 344, 343, 343, 342, and 342 nm, respectively (Fig. 3a, inset). Furthermore, the hydrodynamic diameter, Φ_H, of securin also decreased with the progression of the folding process. The particle sizes from the unfolded to the folded state were 10.8 ± 0.36, 8.38 ± 0.25, 6.68 ± 0.21, 5.96 ± 0.01, 5.84 ± 0.02, and 5.21 ± 0.12 nm (Fig. 3b). These results indicate that the securin protein approaches its native structure following the on-path folding process. Figure 3c shows the CD profiles of the folded state and folding reaction intermediates of securin at wavelengths from 200 to 260 nm. Based on the smooth profiles of the securin protein in the CD spectra, we conclude that there is no or minimal secondary structure formation in securin during the folding process.

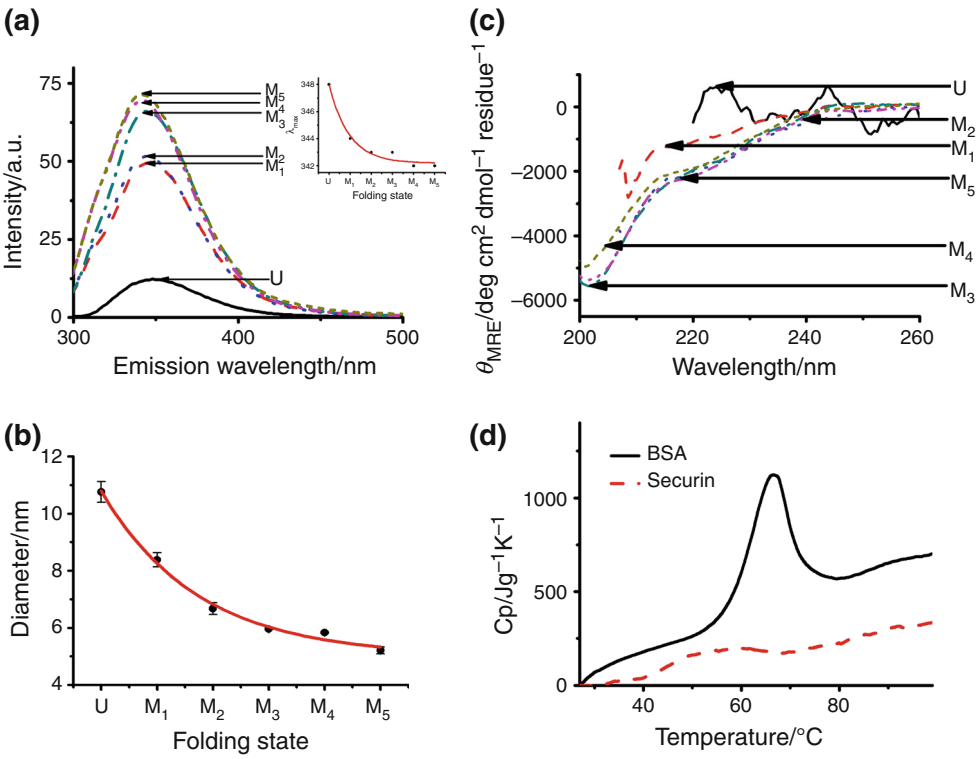

Fig. 3 Analysis of structural features of on-path folding reaction intermediates of securin. **a** The fluorescence spectra of U, M_1, M_2, M_3, M_4, and M_5 of securin are indicated in the figure. **b** Particle size of folding reaction intermediates of securin, analyzed by DLS. **c** Secondary structure analysis of securin at 20 °C. The CD curves of reaction intermediate states U, M_1, M_2, M_3, M_4, and M_5 have been marked in the figure. **d** Thermal stability analysis of folded securin. The temperature dependence of the specific heat capacity of folded securin (*dashed line*) in Tris buffer, and that of BSA (regular protein control; *solid line*) are shown

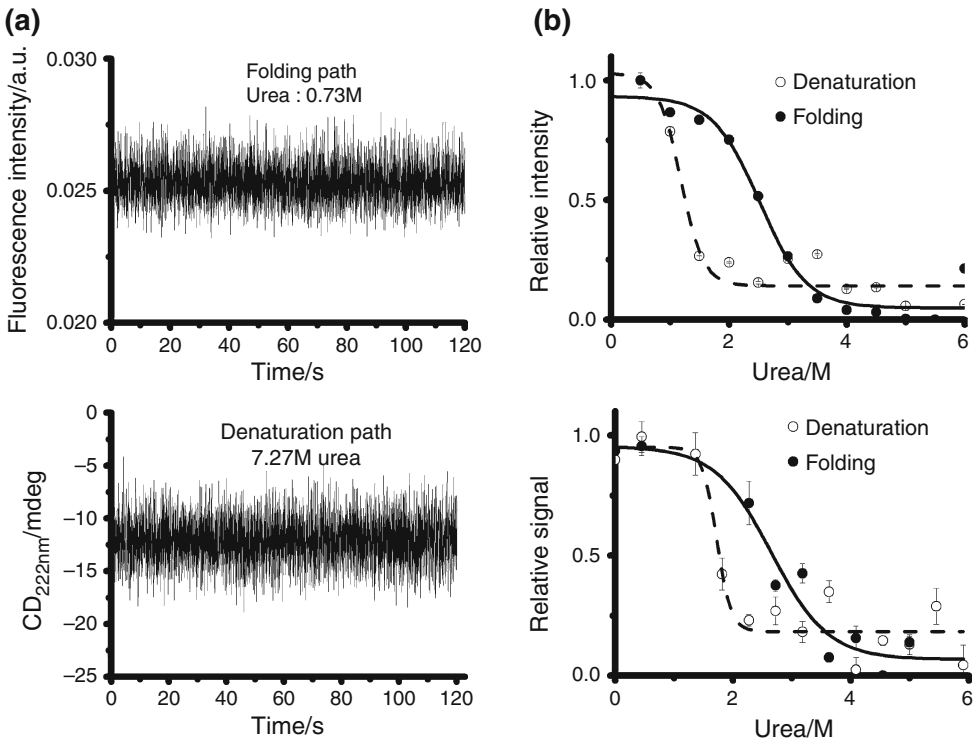

Fig. 4 Folding/unfolding analysis based on kinetics and equilibrium experiments of securin. **a** Folding kinetic analysis of fluorescence signal (*upper panel*) and CD signal at 222 nm (*lower panel*) of securin from the stopped-flow experiments. **b** Intrinsic fluorescence at 342 nm (*upper panel*) and CD signal at 222 nm (*lower panel*) of securin at different urea concentrations in the equilibrium reaction

Thermal stability analysis of securin

Protein stability can be measured by DSC [30, 31]. We used DSC to investigate the thermal stability of folded securin. The DSC profiles of folded securin from 25 to 95 °C showed a tiny thermal transition signal in the folded state (Fig. 3d). In contrast, a clear phase transition peak can be observed in the case of BSA (Fig. 3d), a regular protein. The melting temperatures of securin and BSA are 53.6 and 66.1 °C, and their enthalpy change (ΔH) values are 29.31 and 884.88 kJ mol^{-1}, respectively. In order to rule out faulty measurements by DSC, BSA was used as a positive control (Fig. 3d).

Folding kinetics and equilibrium analysis of securin unfolding/folding

The observed reaction rate (K_{obs}) of securin cannot be determined by stopped-flow analyses, because of the unchanging signal in intrinsic fluorescence (Fig. 4a, upper panel) and CD (Fig. 4a, lower panel) measurements. The undetectable K_{obs} indicated that both folding and unfolding rates are too fast to be detected. To ensure the folding dynamics of securin, equilibrium unfolding/folding experiments were performed, using measurements of intrinsic fluorescence at 342 nm and CD at 222 nm. For the unfolding process, $[Urea]_{50\ \%}$ is 1.72 and 1.18 M; m-value is 20.41 and 12.78 kJ mol^{-1} K^{-1}; and $\Delta G^{H_2O}_{f-u}$ is −35.1 and −15.08 kJ mol^{-1}, as measured by CD and intrinsic fluorescence measurements, respectively. For the folding process, $[Urea]_{50\ \%}$ is 2.66 and 2.52 M; m-value is 5.18 and 6.26 kJ mol^{-1} K^{-1}; and $\Delta G^{H_2O}_{f-d}$ is −13.78 and −15.78 kJ mol^{-1} based on CD and intrinsic fluorescence measurements, respectively. Accordingly, there is a hysteresis path in the folding/unfolding reactions at equilibrium.

Discussion

The amount of securin is extremely low under native physiological conditions and it is not easy to collect sufficient amounts for folding dynamics and kinetics studies. Therefore, we overexpressed recombinant human securin protein in *E. coli* and collected it from inclusion bodies. However, the aggregated protein consisted of both misfolded and folded protein, and its functional structure needed to be recovered by a protein folding process [20, 23, 24]. By applying three different folding paths, both intrinsic fluorescence and particle size analysis are shown in Fig. 1, indicated that securin could fold into a compact conformation by an on-path folding process. This folded securin could bind with its interaction target, p53 [16] (Fig. 2), indicating that the folded securin was functional. In other words, the on-path folding process used in this study was suitable for securin folding.

As the on-path folding reaction progressed, an increase in intrinsic fluorescence and reduction in particle size could be observed in the folding reaction intermediates (molten globule state [32, 33]; Fig. 3a, b). These results indicate that the intrinsic fluorescence and particle size of securin may be affected by the solvent environment. The CD analysis shown in Fig. 3c indicates that securin contains no or minimal secondary structure. Furthermore, DSC was used to analyze the thermal stability of securin. As seen in Fig. 3d, the heat capacity of folded securin changes slowly and this takes place over a large temperature range. This phenomenon is similar to that of the glass transition profile seen in DSC experiments [34]. In DSC measurements, the glass transition is defined as the temperature at which the change of state of amorphous material from a glassy state to a rubbery state occurs [35]. However, both the glassy and rubbery states are non-crystalline states. Owing to the amorphous structure, the glass transition of non-crystalline material is not fixed and occurs in local motion [34]. Accordingly, the free energy changes during the glass transition are weak and slow. DSC measurements of the glass transition-like profile of thermal denaturation of securin indicate that the enthalpy change of securin is very weak during the thermal denaturing process. In other words, the free energy differences between the folded and unfolded states on the protein's folding landscape are very small.

The K_{obs} of kinetic unfolding/folding reactions of securin cannot be detected in stopped-flow analysis (Fig. 4a); this also indicates that the folding/unfolding rates are too fast to be detected. In other words, securin is particularly sensitive to its solvent environment. Therefore, hysteresis profiles can be observed in equilibrium folding/unfolding experiments in this study (Fig. 4b). This result also supports the notion that the folding reaction of securin is not a simple two-state transition.

In summary, this is the first IDP folding study using thermodynamics and kinetics approaches. Moreover, securin is an IDP that needs an appropriate folding process to restore its function. Folded securin may have a compact hydrophobic core and conformation, but it contains very weak tertiary interactions and no secondary structure. Moreover, securin is sensitive to its solvent environment. Hence, its folding route is different to its unfolding route. The research approach used in this study may be used in the analysis and/or identification of IDPs in future studies.

Acknowledgements We would like to thank the National Synchrotron Radiation Research Center for providing the CD spectrophotometer used in this study. This study was supported in part by grants NSC 97-2112-M-009-009-YM3 and NSC 100-2112-M-009-004-MY3, Taiwan, R.O.C.

References

1. Ward JJ, Sodhi JS, McGuffin LJ, Buxton BF, Jones DT. Prediction and functional analysis of native disorder in proteins from the three kingdoms of life. J Mol Biol. 2004;337:635–45.
2. Wright PE, Dyson HJ. Intrinsically unstructured proteins: reassessing the protein structure-function paradigm. J Mol Biol. 1999;293:321–31.
3. Jin S, Martinek S, Joo WS, Wortman JR, Mirkovic N, Sali A, et al. Identification and characterization of a p53 homologue in Drosophila melanogaster. Proc Natl Acad Sci USA. 2000;97:7301–6.
4. Mark W-Y, Liao JCC, Lu Y, Ayed A, Laister R, Szymczyna B, et al. Characterization of segments from the central region of BRCA1: an intrinsically disordered scaffold for multiple protein–protein and protein-DNA interactions? J Mol Biol. 2005;345:275–87.
5. Dunker AK, Obradovic Z. The protein trinity–linking function and disorder. Nat Biotech. 2001;19:805–6.
6. Dunker AK, Lawson JD, Brown CJ, Williams RM, Romero P, Oh JS, et al. Intrinsically disordered protein. J Mol Graph Model. 2001;19:26–59.
7. Csizmok V, Felli IC, Tompa P, Banci L, Bertini I. Structural and dynamic characterization of intrinsically disordered human securin by NMR spectroscopy. J Am Chem Soc. 2008;130:16873–9.
8. Zou H, McGarry TJ, Bernal T, Kirschner MW. Identification of a vertebrate sister-chromatid separation inhibitor involved in transformation and tumorigenesis. Science. 1999;285:418–22.
9. Zhou Y, Mehta KR, Choi AP, Scolavino S, Zhang X. DNA damage-induced inhibition of securin expression is mediated by p53. J Biol Chem. 2003;278:462–70.
10. Romero F, Gil-Bernabe AM, Saez C, Japon MA, Pintor-Toro JA, Tortolero M. Securin is a target of the UV response pathway in mammalian cells. Mol Cell Biol. 2004;24:2720–33.
11. Christopoulou L, Moore JD, Tyler-Smith C. Over-expression of wild-type securin leads to aneuploidy in human cells. Cancer Lett. 2003;202:213–8.
12. Romero F, Multon M-C, Ramos-Morales F, Dominguez A, Bernal JA, Pintor-Toro JA, et al. Human securin, hPTTG, is associated with Ku heterodimer, the regulatory subunit of the DNA-dependent protein kinase. Nucl Acids Res. 2001;29:1300–7.
13. Ogbagabriel S, Fernando M, Waldman FM, Bose S, Heaney AP. Securin is overexpressed in breast cancer. Mod Pathol. 2005;18:985–90.
14. Mitsuhiro Y. Cell cycle mechanisms of sister chromatid separation; roles of Cut1/separin and Cut2/securin. Genes Cells. 2000;5:1–8.
15. Wang Z, Yu R, Melmed S. Mice lacking pituitary tumor transforming gene show testicular and splenic hypoplasia, thymic hyperplasia, thrombocytopenia, aberrant cell cycle progression, and premature centromere division. Mol Endocrinol. 2001;15:1870–9.
16. Bernal JA, Luna R, Espina A, Lazaro I, Ramos-Morales F, Romero F, et al. Human securin interacts with p53 and modulates p53-mediated transcriptional activity and apoptosis. Nat Genet. 2002;32:306–11.
17. Fuxreiter M, Tompa P, Follis A, Galea C, Kriwacki R. Intrinsic protein flexibility in regulation of cell proliferation: advantages for signaling and opportunities for novel therapeutics. Adv Exp Med Biol. 2012;725:27–49.
18. Chang CC, Lin CS, Chen MC, Liu YC, Huang YF, Lin PY, et al. Folding and structural characterization of recombinant cyclin-dependent kinase inhibitor $p21^{(Cip1,\ Waf1,\ Sdi1)}$. Biophys Rev Lett. 2006;1:45–56.

19. Chang C-C, Lin P-Y, Yeh X-C, Deng K-H, Ho Y-P, Kan L-S. Protein folding stabilizing time measurement: a direct folding process and three-dimensional random walk simulation. Biochem Biophys Res Commun. 2005;328:845–50.
20. Chang C-C, Yeh X-C, Lee H-T, Lin P-Y, Kan L-S. Refolding of lysozyme by quasistatic and direct dilution reaction paths: a first-order-like state transition. Phys Rev E. 2004;70:011904.
21. Liu Y-L, Lee H-T, Chang C-C, Kan L-S. Reversible folding of cysteine-rich metallothionein by an overcritical reaction path. Biochem Biophys Res Commun. 2003;306:59–63.
22. Chang C-C, Cheng M-S, Su Y-C, Kan L-S. A first-order-like state transition for recombinant protein folding. J Biomol Struct Dyn. 2003;21:247–55.
23. Chang C-C, Tsai C-T, Chang C-Y. Structural restoration of inactive recombinant fish growth hormones by chemical chaperonin and solvent restraint approaches. Protein Eng. 2002;15:437–41.
24. Chang C-C, Su Y-C, Cheng M-S, Kan L-S. Protein folding by a quasi-static-like process: a first-order state transition. Phys Rev E. 2002;66:021903.
25. Tzang B-S, Lai Y-C, Hsu M, Chang H-W, Chang C-C, Huang PC, et al. Function and sequence analyses of tumor suppressor gene p53 of CHO.K1 cells. DNA Cell Biol. 1999;18:315–21.
26. Taheri-Kafrani A, Bordbar A-K. Isothermal titration calorimetric study on the interaction of apo-human transferrin with sodium *n*-dodecyl sulfate. J Therm Anal Calorim. 2013. doi:10.1007/s10973-013-3342-6.
27. Nicoli DF, Hasapidis K, O'Hagan P, McKenzie DC, Wu JS, Chang YJ et al. High-resolution particle size analysis of mostly submicrometer dispersions and emulsions by simultaneous combination of dynamic light scattering and single-particle optical sensing. Particle Size Distribution III. ACS Symposium Series: American Chemical Society; 1998. p. 52–76.
28. Nölting B. Protein Folding Kinetics: Biophysical Methods. New York: Springer, Berlin Heidelberg; 2005.
29. Panda D, Datta A. Evidence for covalent binding of epicocconone with proteins from synchronous fluorescence spectra and fluorescence lifetimes. J Chem Sci. 2007;119:99–104.
30. Fekecs Tamás, Zapf István, Ferencz Andrea, Lőrinczy D. Differential scanning calorimetry (DSC) analysis of human plasma in melanoma patients with or without regional lymph node metastases. J Therm Anal Calorim. 2013;108:149–52.
31. Kamiyama T, Tanaka T, Satoh M, Kimura T. Destabilization of cytochrome c by modified β-cyclodextrin. J Therm Anal Calorim. 2013;113:1491–6.
32. Ptitsyn O. How molten is the molten globule? Nat Struct Biol. 1996;3:488–90.
33. Ptitsyn OB. Kinetic and equilibrium intermediates in protein-folding. Protein Eng. 1994;7:593–6.
34. Meste ML, Champion D, Roudaut G, Blond G, Simatos D. Glass transition and food technology: a critical appraisal. J Food Sci. 2002;67:2444–58.
35. Labuza TP, Hyman CR. Moisture migration and control in multi-domain foods. Trends Food Sci Technol. 1998;9:47–55.